

Dynamics of a superlattice with an impurity in an ac electric field

Ai-Zhen Zhang,^{1,2} Ping Zhang,³ Duan Suqing,⁴ Xian-Geng Zhao,⁴ and Jiu-Qing Liang^{1,2}

¹*Institute of Physics and Center for Condensed Matter Physics, Chinese Academy of Sciences, P.O. Box 603-12, Beijing 100080, China*

²*Institute of Theoretical Physics, Shanxi University, Taiyuan 030006, China*

³*Graduate School, China Academy of Engineering Physics, P.O. Box 2101, Beijing 100088, China*

⁴*Institute of Applied Physics and Computational Mathematics, P.O. Box 8009, Beijing 100088, China*

(Received 11 July 2000; published 9 January 2001)

Within a single-band tight-binding model, we investigate the dynamics of a one-dimensional semiconductor superlattice with an impurity under the action of an ac electric field. The long-time mean-square displacement is analytically obtained and the quasienergy spectrum is numerically calculated. We find that although the dynamic localization condition is not destroyed by the impurity, the quasienergy spectrum and corresponding local dynamics of the system are tuned dramatically by the ratio of the impurity potential to the ac field frequency. In particular, when the ratio becomes an integer, avoided crossing in the quasienergy spectrum occurs and the dynamics of the system is dominated by resonant oscillations between the impurity and its two nearest-neighbor sites. Such an effect is more favorable for experimental investigations of coherent oscillations of charged carriers.

DOI: 10.1103/PhysRevB.63.045319

PACS number(s): 73.21.-b, 72.15.Rn, 63.20.Kr

In recent years, there has been growing interest in the response of semiconductor superlattices to high-frequency ac electric fields¹⁻⁸ because the availability of high-quality semiconductor superlattices facilitates some interesting experimental studies. In the investigation of electron evolution in such a system within the tight-binding approximation, it is found that an initially localized particle will remain localized if the ratio of the field magnitude to the field frequency is a root of zeroth order Bessel function.⁹ This phenomenon has been called dynamic localization and was later found to be related to the effect of band collapse of the quasienergy miniband,¹⁰ which has been verified experimentally in an optical lattice.¹¹ However, since fabrication is not always perfect, irregularities in the height or width of the barriers or wells and other kinds of defects are inevitably introduced into the actual superlattice systems. So, another step in the direction of more realistic models should be the investigation of the effect of various disorders. Recently considerable attention have been devoted to some models which contain different kinds of disorders,¹²⁻¹⁶ such as the Kronig-Penney model, Aubry model, Harper model, Fibonacci model, and Thue-Morse model.

In this paper we investigate the dynamics of a one-dimensional system with an impurity under the action of an ac electric field. By studying the long-time behavior of the mean-square displacement we analytically obtain the dynamic localization condition, which is the same as that of perfect lattice. To further study the effects of the impurity on the dynamics of the system, we numerically calculate the quasienergy spectrum with the help of the Floquet formalism. We find that the Floquet states of the system undergo a series of avoided crossings, at which remarkable changes in the dynamic behavior of the system occur; this is reflected by the complete resonant oscillations between the impurity and its two nearest-neighbor sites. Such an effect may have important device applications for generating electromagnetic radiation.

We consider a single-band tight-binding model of a one-dimensional system with an impurity at site 0 in an ac electric field $E(t) = E \cos(\omega t)$. The corresponding Hamiltonian in the Wannier representation can be written as

$$H = \sum_n V(|n\rangle\langle n+1| + |n+1\rangle\langle n|) + \varepsilon_0|0\rangle\langle 0| - eaE \cos(\omega t) \sum_n n|n\rangle\langle n|, \quad (1)$$

where V is the nearest-neighbor hopping matrix element, e is the charge of the particle, a is the lattice constant, ε_0 is the impurity potential, E is the amplitude of the ac electric field, ω is the ac field frequency, and $|n\rangle$ represents a Wannier state localized at lattice site n . In the numerical calculations below, we chose $n = 0, \pm 1, \pm 2, \dots, \pm 25$, i.e., the size of the lattice is 51, which approximates a realistic model.

To elucidate the role the impurity plays in coherent dynamics, we first investigate the dynamic localization condition of this system. By expressing the particle state $|\psi(t)\rangle$ as a linear combination of Wannier states $|n\rangle$, i.e., $|\psi(t)\rangle = \sum_n c_n(t)|n\rangle$, one obtains from Eq. (1) the following evolution equation for the amplitude propagators $c_n(t)$ (we put $\hbar = 1$ throughout this paper)

$$i \frac{d}{dt} c_n(t) = V(c_{n+1}(t) + c_{n-1}(t)) + \varepsilon_0 c_0(t) \delta_{n,0} - neaE f(t) c_n(t). \quad (2)$$

For convenience we have written the quantity $\cos(\omega t)$ as $f(t)$. By scaling $\tau = 2Vt$, $\epsilon = \varepsilon_0/2V$, $\alpha = eaE/2V$, and introducing

$$c_n(\tau) = D_n(\tau) e^{in\theta(\tau)}, \quad \theta(\tau) = \alpha \int_0^\tau d\tau' f(\tau'), \quad (3)$$

we have

$$i\frac{d}{d\tau}D_n(\tau) = \frac{1}{2}[D_{n+1}(\tau)e^{i\theta(\tau)} + D_{n-1}(\tau)e^{-i\theta(\tau)}] + \epsilon D_0(\tau)\delta_{n,0}. \quad (4)$$

In solving Eq. (4), we perform a discrete Fourier transform along the chain defined by $D(k, \tau) = \sum_n D_n(\tau) \exp(-ink)$. The form of Eq. (4) in k space is then

$$i\frac{\partial}{\partial\tau}D(k, \tau) = \cos[k + \theta(\tau)]D(k, \tau) + \epsilon D_0(\tau). \quad (5)$$

We assume that the particle is initially localized at the impurity site, i.e., $c_n(0) = \delta_{n,0}$, the solution of Eq. (5) for this initial condition is therefore presented as

$$D(k, \tau) = \exp\left(-i\int_0^\tau d\tau' \cos[k + \theta(\tau')]\right) - i\epsilon \int_0^\tau d\tau' D_0(\tau') \times \exp\left(-i\int_{\tau'}^\tau dx \cos[k + \theta(x)]\right). \quad (6)$$

By defining

$$\mu(\tau) = \int_0^\tau dx \cos \theta(x), \quad \sigma(\tau) = \int_0^\tau dx \sin \theta(x), \quad (7)$$

$$\mu(\tau, \tau') = \mu(\tau) - \mu(\tau'), \quad \sigma(\tau, \tau') = \sigma(\tau) - \sigma(\tau'), \quad (8)$$

$$z(\tau, \tau') = \sqrt{\mu^2(\tau, \tau') + \sigma^2(\tau, \tau')}, \quad \Phi(\tau, \tau') = \tan^{-1} \frac{\sigma(\tau, \tau')}{\mu(\tau, \tau')}, \quad (9)$$

we get the following Volterra integral equation of the second kind for the amplitude propagator of the initially occupied site 0

$$D_0(\tau) = J_0(z(\tau)) - i\epsilon \int_0^\tau d\tau' J_0(z(\tau, \tau')) D_0(\tau'), \quad (10)$$

and amplitude propagators at any site n ,

$$D_n(\tau) = (-i)^n \left\{ J_{-n}(z(\tau)) e^{-in\Phi(\tau)} - i\epsilon \int_0^\tau d\tau' D_0(\tau') \times J_n(z(\tau, \tau')) e^{-in\Phi(\tau, \tau')} \right\}, \quad (11)$$

where J_n is the ordinary Bessel function. Replacing $f(t)$ with $\cos(\omega t)$ leads to

$$\theta(\tau) = \frac{\alpha}{\beta} \sin(\beta\tau), \quad \beta = \omega/2V, \quad (12)$$

$$z(\tau, \tau') = |\mu(\tau, \tau') + i\sigma(\tau, \tau')| = \left| J_0(\alpha/\beta)(\tau - \tau') + \sum_{l \neq 0} J_l(\alpha/\beta) \frac{\exp(il\beta\tau) - \exp(il\beta\tau')}{il\beta} \right|. \quad (13)$$

We consider the long-time evolution behavior of the charged particle. Taking the limit $\tau \rightarrow \infty$ in Eq. (10), we have

$$D_0(\tau \rightarrow \infty) = \lim_{\tau \rightarrow \infty} \left\{ J_0(J_0(\alpha/\beta)\tau) - i\epsilon \int_0^\tau d\tau' D_0(\tau') \times J_0(J_0(\alpha/\beta)(\tau - \tau')) \right\}. \quad (14)$$

Equation (14) can be solved exactly as

$$D_0(\tau \rightarrow \infty) = a(\tau \rightarrow \infty) + ib(\tau \rightarrow \infty), \quad (15)$$

with

$$a(\tau) = J_0(J_0(\alpha/\beta)\tau) - \frac{\epsilon^2}{\sqrt{J_0^2(\alpha/\beta) + \epsilon^2}} \int_0^\tau d\tau' \times J_0(J_0(\alpha/\beta)\tau') \sin[\sqrt{J_0^2(\alpha/\beta) + \epsilon^2}(\tau - \tau')], \quad (16)$$

$$b(\tau) = -\frac{\epsilon}{\sqrt{J_0^2(\alpha/\beta) + \epsilon^2}} \sin[\sqrt{J_0^2(\alpha/\beta) + \epsilon^2}\tau]. \quad (17)$$

This leads to

$$|D_0(\tau \rightarrow \infty)|^2 = \frac{\epsilon^2}{J_0^2(\alpha/\beta) + \epsilon^2}. \quad (18)$$

Considering the fact that $\sigma(\tau)$ is periodic with the period $2\pi/\beta$, $\mu(\tau \rightarrow \infty) = J_0(\alpha/\beta)\tau$, $z(\tau \rightarrow \infty) = J_0(\alpha/\beta)\tau$, and $\phi(\tau \rightarrow \infty) = 0$, the mean-square displacement $\langle n^2 \rangle (= \sum_n n^2 |c_n(t)|^2)$ can be obtained as

$$\langle n^2 \rangle(\tau \rightarrow \infty) = \frac{1}{2} J_0^2(\alpha/\beta) \tau^2. \quad (19)$$

From Eq. (19) we can see that if $J_0(eaE/\omega) \neq 0$, the mean-square displacement increases without bounds, indicating that an initially localized particle delocalizes. Only if $J_0(eaE/\omega) = 0$, the particle does not escape to infinity. So the dynamic localization condition is that the ratio of eaE/ω is a root of J_0 , i.e., $J_0(eaE/\omega) = 0$. This result is illustrated in Fig. 1, where the self-propagator $\psi_0(t) (= |c_0(t)|^2)$ and the mean-square displacement $\langle n^2 \rangle$ are plotted as functions of dimensionless time ωt with $V/\omega = 0.05$ and $\epsilon_0/\omega = 1$. We plot in Fig. 1(a) the self-propagator for $eaE/\omega = 2.405$ (the first root of J_0) and $eaE/\omega = 1.5$. The corresponding plots of the mean-square displacement are in Fig. 1(b). We can see clearly in Fig. 1(a) that in the case of $eaE/\omega = 1.5$, the recurrences of the self-propagator are incomplete and the suc-

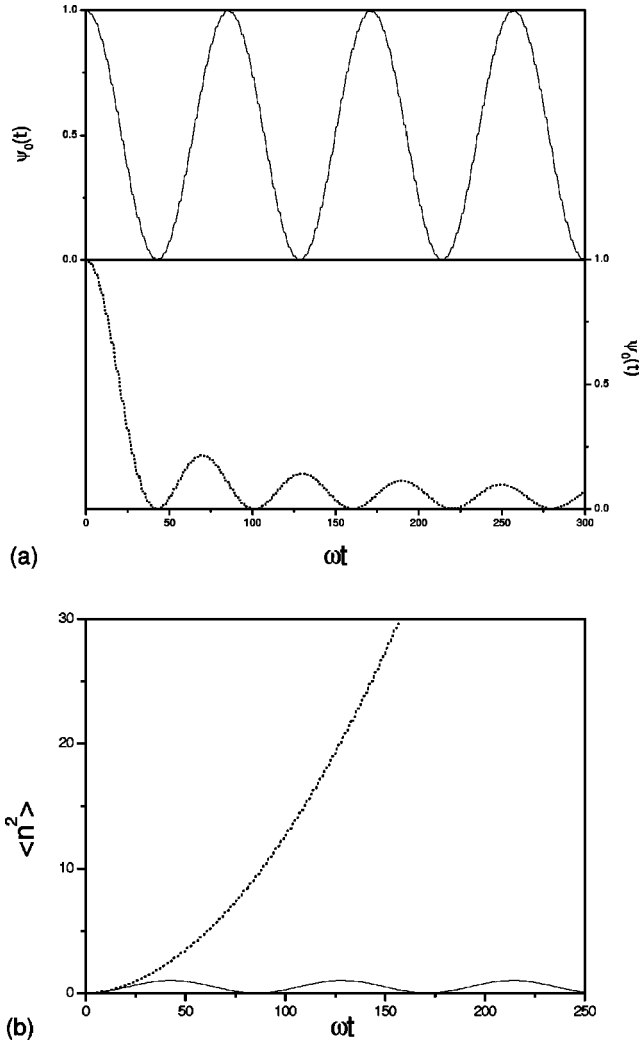


FIG. 1. (a) The self-propagator $\psi_0(t)$ and (b) the mean-square displacement $\langle n^2 \rangle$ as functions of dimensionless time ωt , respectively, for $eaE/\omega = 2.405$ and $eaE/\omega = 1.5$, where $\varepsilon_0/\omega = 1$ and $V/\omega = 0.05$. The solid line corresponds to $eaE/\omega = 2.405$ and the dotted line corresponds to $eaE/\omega = 1.5$.

cessive peaks decrease in magnitude, meaning the escape of the particle. In the case of $eaE/\omega = 2.405$, the self-propagator oscillates between 0 and 1, showing that the particle returns repeatedly to the initially occupied site. All these are also evident from Fig. 1(b) where the mean-square displacement is seen to be bounded and periodic in the case of $eaE/\omega = 2.405$ and grows rapidly in the case of $eaE/\omega = 1.5$. We can conclude that whenever eaE/ω does not equal to 2.405, delocalization occurs.

The above analytical and numerical calculations suggest the same dynamic localization condition for a superlattice with an impurity as that without the impurity. It does not mean that the appearance of an impurity has no influence on the dynamic behavior of the system. In fact, the breakdown of the spatial translation symmetry should have fundamental effects on the local dynamics of the system. This is reflected by the quasienergy spectrum given below. For a numerical calculation of quasienergies it is convenient to introduce the time-evolution operator $U(t,0)$, which satisfies the equation

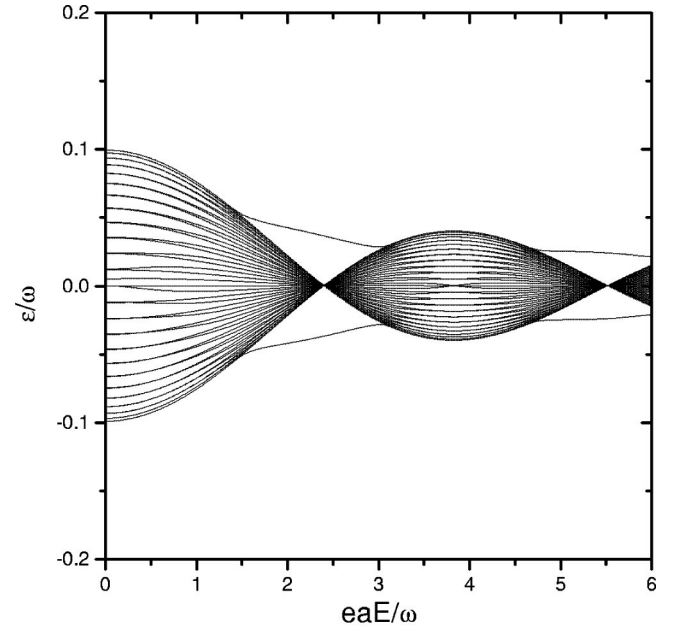


FIG. 2. Quasienergy band ε/ω plotted versus eaE/ω , where $\varepsilon_0/\omega = 1$ and $V/\omega = 0.05$.

$$i\frac{\partial}{\partial t}U(t,0) = H(t)U(t,0) \quad (20)$$

with the initial condition $U(0,0) = 1$. The time periodicity of the Hamiltonian (1) enables us to describe the quantum evolution process of the system in terms of the Floquet theory. Within the framework of the Floquet formalism we can get

$$[U(T,0) - e^{-i\varepsilon T}]\psi(0) = 0. \quad (21)$$

Thus, the quasienergies and Floquet states can be determined directly so long as we numerically integrate Eq. (21) over one period and diagonalize $U(T,0)$. Figure 2 shows the numerical result of the quasienergy band ε/ω as a function of eaE/ω , where other parameters are the same as those employed in Fig. 1. We can see because of the influence of the impurity, there are two quasienergies that behave differently from the rest of the miniband which, with increasing value of eaE/ω , oscillates in width and collapses at values of eaE/ω equal to a zero of the Bessel function J_0 just as the case of perfect lattice. This is in agreement with the analytical result obtained above. In order to see clearly the effect of the impurity on the quasienergy spectrum, we plot in Fig. 3 one Brillouin zone $-\frac{1}{2} \leq \varepsilon/\omega \leq \frac{1}{2}$ of quasienergies versus ε_0/ω , where $V/\omega = 0.05$ and $eaE/\omega = 2.405$. It shows in Fig. 3 that whenever the ratio of the impurity potential to the ac field frequency becomes an integer, avoided crossing occurs between two quasienergies, and its splitting amplitude decreases with increasing integer value of ε_0/ω . Other quasienergies present degeneracy.

To understand the underlying physics caused by the avoided crossings indicated in Fig. 3, we show in Figs. 4(a)–4(d) the time evolution of $\psi_0(t)$, $\psi_{-1}(t)$, and $\psi_1(t)$ for different values of ε_0/ω or V/ω with $eaE/\omega = 2.405$. Figure 4(a) shows the case for perfect lattice with $V/\omega = 0.05$. We

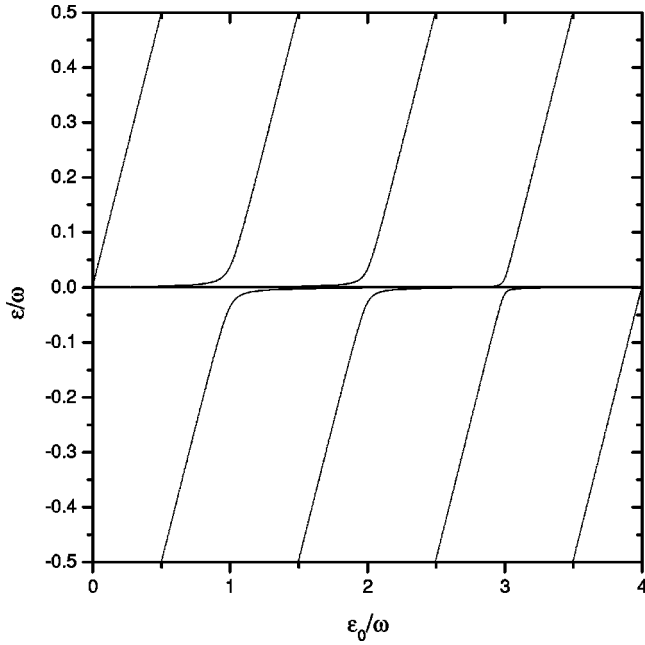


FIG. 3. One Brillouin zone $-\frac{1}{2} \leq \varepsilon/\omega \leq \frac{1}{2}$ of quasienergies as functions of ε_0/ω , where $eaE/\omega = 2.405$ and $V/\omega = 0.05$.

can see the particle is almost localized at its initially occupied site. Figure 4(b) shows the case for $\varepsilon_0/\omega = 1.2$ and $V/\omega = 0.05$, i.e., far from the avoided crossings. It is clear that the particle has a tendency towards localization similar to that of Fig. 4(a). We plot in Fig. 4(c) the case for $\varepsilon_0/\omega = 1$ and $V/\omega = 0.05$, corresponding to the avoided crossing of quasienergies. We can see that the oscillations are quite different from that shown in Figs. 4(a) and 4(b). The self-propagator $\psi_0(t)$ oscillates between 0 and 1 and the maximum occupation of the sites 1 and -1 is 0.5, which corresponds to site 0 occupation of 0. We also notice that the probability propagators for site 1 [i.e., $\psi_1(t)$] and -1 [i.e., $\psi_{-1}(t)$] are the same and the oscillations are in-phase. This complete oscillation between the sites 0 and ± 1 can be understood in an effective three-level model, in which the site states $|0\rangle$, $|1\rangle$, and $|-1\rangle$ is three localized basis functions [the inset in Fig. 4(c)].

In the present calculation because the site-energy difference between the impurity and its two nearest neighbors is ω , and the coupling parameter V is relatively small compared to the driving frequency, the detuning between the site state $|0\rangle$ and two lower states $|1\rangle$ and $|-1\rangle$ is negligible. In this case we come to the familiar one-photon resonance of a three level system, which is equivalent to a simple three-site Rabi oscillation. To support this point of view, we have truncated the Hamiltonian (1) to include only three sites ($n = \pm 1$) and calculated the time evolution of the reduced system with the same parameters used in Fig. 4(c). We find that the result is exactly identical to that shown in Fig. 4(c) (not depicted here). With increasing value of V/ω , the energy detuning between the sites 0 and ± 1 cannot be neglected and there will be three intrinsic frequencies involving in the dynamics of the system, so the complete Rabi oscillation between the three sites will be break down. We give an example in Fig.

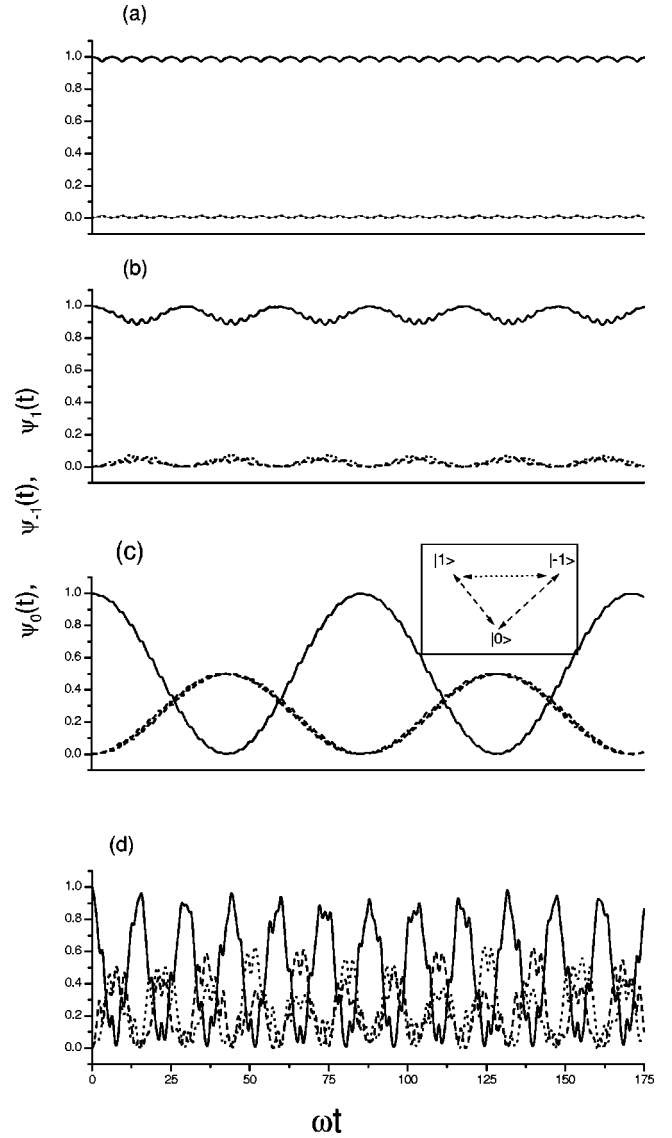


FIG. 4. $\psi_0(t)$, $\psi_{-1}(t)$, and $\psi_1(t)$ are plotted as functions of dimensionless time ωt for different values of ε_0/ω or V/ω , (a) $\varepsilon_0/\omega = 0$ and $V/\omega = 0.05$, (b) $\varepsilon_0/\omega = 1.2$ and $V/\omega = 0.05$, (c) $\varepsilon_0/\omega = 1$ and $V/\omega = 0.05$, and (d) $\varepsilon_0/\omega = 1$ and $V/\omega = 0.2$. The solid line corresponds to site 0, the dashed line corresponds to site -1 , and the dotted line corresponds to site 1.

4(d) with $V/\omega = 0.2$ and other parameters are the same as for Fig. 4(c). We can see clearly that the deviation from the case of zero detuning leads to out-of-phase oscillations of the site states $|1\rangle$ and $|-1\rangle$. This, together with the coupling to the impurity state, yields the complex dynamic behavior shown in Fig. 4(d).

Figures 4(a)–4(d) show that the systematic appearance of avoided crossings in the quasienergy spectrum is related to fundamental changes of the dynamic behavior of the system and we can control the complicated oscillatory behavior of the system by varying the value of V/ω . When the dynamic localization condition is satisfied, as well as the system parameters are appropriately chosen to be at the avoided crossings, strong transition occurs and the dynamics of the system

is dominated by resonant oscillations between the impurity and its two nearest-neighbor sites.

In conclusion, making use of analytic and numerical calculations we have investigated the dynamics of a superlattice with an impurity driven by an ac electric field. We find that the interplay of the ac electric field and the impurity results in remarkable feature occurring in such a system. The dynamic effect is dramatically tuned by the ratio of the impurity potential to the ac field frequency. In particular, when the ratio is an integer, resonant oscillations can take place between the impurity and its two nearest-neighbor sites,

which is manifested as an avoided crossing in the quasienergy spectrum. Therefore, it is more favorable for observing coherent oscillations in experiments. From this point of view it will be interesting to study ac-driven superlattices with intentionally introduced disorder.

This work was supported in part by the National Natural Science Foundation of China under Grant No. 19725417, the National PAN-DENG Project under Grant No. 95-YU-41, and a grant of the China Academy of Engineering and Physics.

-
- ¹J. Rotvig, A.-P. Jauho, and H. Smith, *Phys. Rev. Lett.* **74**, 1831 (1995); *Phys. Rev. B* **54**, 17 691 (1996).
- ²X.-G. Zhao, G.A. Georgakis, and Q. Niu, *Phys. Rev. B* **54**, R5235 (1996); **56**, 3976 (1997).
- ³M. Holthaus and D.W. Hone, *Phys. Rev. B* **47**, 6499 (1993); **49**, 16 605 (1994).
- ⁴P.S.S. Guimarães, B. J. Keay, J. P. Kaminski, S. J. Allen, P. F. Hopkins, A. C. Gossard, L. T. Florez, and J. P. Harbison, *Phys. Rev. Lett.* **70**, 3792 (1993).
- ⁵T. Meier, G. Vopplissen, P. Thomas, and S.W. Koch, *Phys. Rev. B* **51**, 14 490 (1995).
- ⁶K.N. Alekseev and G.P. Berman, *Phys. Rev. B* **54**, 10 625 (1996).
- ⁷R. Agnado, G. Platero, M. Moscoso, and L.L. Bonilla, *Phys. Rev. B* **55**, R16 053 (1997).
- ⁸B.J. Keay, S. Zeuner, S. J. Allen, K. D. Maranowski, A. C. Gossard, U. Bhattacharya, and M. J. W. Rodwell, *Phys. Rev. Lett.* **75**, 4102 (1995); **75**, 4089 (1995).
- ⁹D.H. Dunlap and V.M. Kenkre, *Phys. Rev. B* **34**, 3625 (1986); X.-G. Zhao, *Phys. Lett. A* **155**, 299 (1991); J. Zak, *Phys. Rev. Lett.* **71**, 2623 (1993); X.-G. Zhao, *J. Phys.: Condens. Matter* **6**, 2751 (1994).
- ¹⁰M. Holthaus, *Phys. Rev. Lett.* **69**, 351 (1992); *Z. Phys. B: Condens. Matter* **89**, 251 (1992).
- ¹¹K.W. Madison, M.C. Fischer, R.B. Diener, Qian Niu, and M.G. Raizen, *Phys. Rev. Lett.* **81**, 5093 (1998).
- ¹²D.W. Hone and M. Holthaus, *Phys. Rev. B* **48**, 15 123 (1993).
- ¹³M. Luban and J.H. Luscombe, *Phys. Rev. B* **34**, 3674 (1986).
- ¹⁴Z.-Q. Zhang and X.-D. Jing, *Phys. Rev. B* **39**, 11 428 (1989).
- ¹⁵P.E. de Brito, C.A.A. da Silva, and H.N. Nazareno, *Phys. Rev. B* **51**, 6096 (1995).
- ¹⁶A.A. Toropov, T. V. Shubina, S. V. Sorokin, A. V. Lebedev, R. N. Kyutt, S. V. Ivanov, M. Karlsteen, M. Willander, G. R. Pozina, J. P. Bergman, and B. Monemar, *Phys. Rev. B* **59**, R2510 (1999).